Bcl-2 is essential for Foeniculum vulgare seed extract-induced apoptosis in lung cancer

Weiwei Ke
Shengjing Hospital of China Medical University
Xiangxuan Zhao (xiangxuanzhao@163.com)
Shengjing Hospital of China Medical University https://orcid.org/0000-0003-1209-9995
Zaiming Lu
Shengjing Hospital of China Medical University

Research

Keywords: Foeniculum vulgare, Lung cancer, Apoptosis, Bcl-2, Chemotherapy

Posted Date: March 23rd, 2020

DOI: https://doi.org/10.21203/rs.3.rs-18625/v1

Abstract

Background

The factors behind the pathogenesis of lung cancer are not clear, and treatment failure is generally caused by drug resistance, recurrence, and metastasis. Development of new therapeutic agents to overcome drug-resistance remains a challenge clinically. Various extracts of Foeniculum vulgare have shown promising anticancer activity; however, effects on lung cancer and the underlying molecular mechanisms of action are not clear.

Methods

The cytotoxicity effects of EEFS were assessed by morphological changes or MTT assay. The BALB/c nude mice xenograft model was used for the in vivo study. Apoptotic ratio assay based on Annexin V-PI staining were measured by flow cytometry. Effect of EEFS on expression of apoptotic proteins was measured by Western blot. Mitochondria toxicity was evaluated by fluorescence to show membrane potential under a fluorescent microscope and Cytochrome C release.

Results

We found that the ethanol extract of Foeniculum vulgare seeds (EEFS) significantly reduced lung cancer cell growth in vitro and in vivo. EEFS decreased the viability of and triggered apoptosis in the lung cancer cell lines NCI-H446 and NCI-H661. EEFS induced apoptosis mainly through inhibition of Bcl-2 protein expression, reduction of mitochondrial membrane potential, and release of Cytochrome C. Moreover, EEFS significantly inhibited colony formation and cell migration in lung cancer cells. EEFS also effectively inhibited the growth of xenograft tumors derived from NCI-446 cells by reducing Bcl-2 protein expression and inducing apoptosis.

Conclusions

Taken together, these findings suggest that EEFS exerts anti-lung cancer activity by targeting the Bcl-2 protein and may have potential as a therapeutic drug for lung cancer.

Background

Lung cancer is a highly malignant tumor type, with the highest incidence and mortality rates in the world [1]. Lung cancer is mainly divided into non-small cell lung cancer (NSCLC) and small cell lung cancer (SCLC). The former accounts for approximately 85% of the total lung cancer incidence rate and most patients are in the late stage at the time diagnosis [2]. SCLC accounts for approximately 14% of all lung cancers, is more aggressive than NSCLC, and is the number one cause of cancer deaths in men and the second highest cause of cancer deaths in women [3]. In the early stage of lung cancer, surgical resection is the main therapeutic strategy; radiotherapy and chemotherapy are often supplemented in the middle and late stages. First-line chemotherapy drugs include cisplatin, carboplatin, and epidermal growth factor

receptor tyrosine kinase inhibitors (EGFR-TKI). In the later stages, resistance and metastasis commonly occur, leading to treatment failure [4, 5]. Therefore, there is an urgent need to identify new treatment regimens for lung cancer.

Fennel, also known as sweet fennel (Foeniculum vulgare), belongs to the Apiaceae family, which is widely distributed worldwide [6]. The chemical components of the fruit of Foeniculum vulgare are mainly comprised of trans-anethole, fenchone, estragole, sterol, glycosides, essential oils, and alkaloids [7]. Two studies showed that extracts of fennel possessed anticancer activity [8, 9]. For example, Singh et al. found that the incidence of skin and forestomach tumors in Swiss albino mice were significantly reduced by feeding the animals fennel seeds [10]. Sara Levorato et al. reported that fennel seed essential oil induced apoptosis in HepG2 liver cancer cells [11]. The chloroform fraction of fennel seeds inhibited the proliferation of MCF-7 cells and induced cell cycle arrest and apoptosis [12]. The fennel compound anethole induced cell cycle arrest and apoptosis in human prostate cancer cells and exhibited antitumor effects [13]. The coumarin extracted from the dried fruits of fennel demonstrated antioxidant effects, promoted the production of inflammatory factors such as interleukin (IL-6) and tumor necrosis factor α (TNF-α), and inhibited the growth of tumor cells [14, 15]. At present, there are no reports of the anti-lung cancer activity of the ethanol extract of Foeniculum vulgare seeds (EEFS), and the underlying molecular mechanisms of its activity remain unknown.

In this study, we determined that EEFS exerted anti-lung cancer activity by inducing apoptosis in lung cancer cells. EEFS effectively inhibited the formation of lung cancer cell clone formation and cell migration. Both in vivo and in vitro experiments confirmed that EEFS exhibited anti-cancer bioactivity by targeting the expression of Bcl-2. Our data indicate that EEFS is worthy of further study for the benefit of patients with lung cancer.

Materials And Methods

Cell culture and Reagents

Human lung cancer cell lines, NCI-H446 (SCLC) and NCI-H661 (NSCLC), were purchased from Keygen Biotechnology Company (Nanjing, China). Cells were cultured in RPMI 1640 (Hyclone, LA, USA) medium containing 10% fetal bovine serum (Hyclone, LA, USA) and antibiotics (penicillin and streptomycin). Cells were maintained in an incubator with 5% CO_2 at 37 °C and saturated humidity. Hoechst 33258 fluorescent dye and Mito-tracker red probe were purchased from Sigma (St. Louis, MO, USA). CellTiter 96 aqueous non-radioactive cell proliferation assay (MTS) cell activity test kit was purchased from Promega (WI, USA). Annexin V-PI apoptosis detection kit was purchased from BD Biosciences (San Diego, CA, USA). Anti-Bak, anti-Bax, anti-Bcl-2, anti-Survivin, anti-Cytochrome C, anti-cleaved Caspase 3 polyclonal primary antibodies, anti-β-actin monoclonal antibody, and anti-rabbit/mouse horseradish peroxidase (HRP) conjugated secondary antibody were purchased from Cell Signaling Technology (Beverly, MA, USA). ABT-263 was purchased from MedChemExpress (NJ, USA).

EEFS Preparation

Fennel dry seeds (250 g) were washed quickly with sterile distilled water once to remove dust and impurities. Then, they were soaked in 75% ethanol at 4 °C for 48 h and the leach solution was obtained by filter paper filtration. The leach solution was transferred to a rotary evaporator and evaporated and concentrated at a low temperature and reduced pressure to obtain a dark green extract. The extract (100 mg) was re-dissolved in 75% ethanol and sterilized with a 0.2 μm needle filter to produce 50 mg/ml EEFS, which was aliquoted into equal parts and stored at 4 °C, without additional substances added. In this study, except for the special statement, all the control groups contained 75% alcohol as the vehicle group.

Hoechst Staining

The cytotoxicity of EEFS was determined by observing changes in nuclear morphology (chromatin condensation or DNA fragmentation). NCI-H446 and NCI-H661 cells were seeded in 6-well plates at a density of 5×10^5 cells/well, and cells in logarithmic growth were treated with EEFS (0–0.8 mg/ml for NCI-H446 cells, 0–1 mg/ml for NCI-H661 cells) for 48 h. Following treatment, Hoechst 33258 (1 μg/ml) was directly added to the culture medium and incubated in the dark for 15 min at room temperature. To measure apoptosis, the morphological changes of the nucleus were observed via inverted fluorescence microscope (Nikon, Japan); six fields were randomly selected and photographed.

Cell Viability Test

Relative cell viability was evaluated by MTS assay. NCI-H446 and NCI-H661 cells were seeded in 96-well plates (5×10^3 cells/well), and when cell density reached 60%, cells were treated with different concentrations of EEFS (0, 0.1, 0.2, 0.4, and 0.8 mg/ml) for 48 h or the same concentration (NCI-H446 cells: 0.8 mg/ml and NCI-H661 cells: 1 mg/ml were set up as effective dose) for different time periods (12, 24, and 48 h). Following treatment, the relative viability (to vehicle control group) of the cells was detected according to the kit manufacturer's instructions. The relative cell viability was calculated using the following formula: relative cell viability (%) = $(1 - (OD_{control} - OD_{treated})/ OD_{control}) \times 100\%$ [16].

Detection Of Apoptosis By Flow Cytometry

Apoptosis was assessed via the detection of phosphatidylserine (PS) exposure and the binding of Annexin V to the surface of the cell membrane, as well as PI nuclear dye exclusion. NCI-H446 and NCI-H661 cells were grown in 6-well plates at a density of 5×10^5 cells/well. When the cells were in the logarithmic growth stage, they were treated with different concentrations of EEFS (0–0.8 mg/ml for NCI-H446 cells, 0–1 mg/ml for NCI-H661 cells) for 48 h or 0.8 mg/ml for 12, 24, or 48 h. After treatment, the cells were collected and stained according to the instructions of the Annexin V-PI apoptosis detection kit.

A FACSCalibur (BD Biosciences, San Diego, CA, USA) was used to detect apoptosis. Cell quest software (BD Biosciences, San Jose, CA, USA) was used to analyze the data and calculate the apoptotic ratio.

Western Blotting

Western blotting was performed in NCI-H446 and NCI-H661 cells as well as tumor tissues from xenograft mice to examine protein levels, based on a previously published method with minor modifications [17]. Briefly, after treatment with EEFS, ABT-263 or EEFS + ABT-263 under various conditions, NCI-H446 and NCI-H661 cells were collected and washed in PBS and then re-suspended in lysis buffer with 1% NP-40 containing protease inhibitor cocktail. The tumor tissues were homogenized in an ice bath. After the tumor tissues or cell cultures were fully lysed, they were centrifuged at 12,000 rpm and 4 °C for 10 min. The supernatants were transferred to new EP tubes and the protein concentration was measured using the Bradford method. After sample preparation, an equal amount of protein (20 μg) was loaded onto polyacrylamide gels for electrophoresis. Following electrophoresis, the proteins were transferred to a polyvinylidene fluoride (PVDF) membrane (Millipore, Stafford, VA, USA) and blocked at room temperature with Tris-Buffered Saline Tween-20 (TBST) containing 5% skim milk for 30 min. Then, the membrane was incubated overnight at 4 °C with bovine serum albumin (BSA) (1:1000) containing a specific first antibody. After washing the membrane 3 times (10 min/time) with PBST, the membrane was incubated with the corresponding second antibody (1:5000) at room temperature for 2 h. In the darkroom, an enhanced chemiluminescence (ECL) luminescent solution (Millipore, Billerica, MA, USA) was used to display the immunoreactive strip, which was further exposed on film.

Mitochondrial Toxicity Test

Mitochondrial toxicity following EEFS treatment was evaluated by membrane potential reduction and Cytochrome C release. Briefly, NCI-H446 cells were seeded in 6-well plates and once in logarithmic growth, the cells were treated with 0.8 mg/ml EEFS for 6, 12, and 24 h. Following treatment, Mito-tracker red probe (500 nM) was directly added into the culture medium and incubated at 37 °C in the dark for 15 min. The changes of mitochondrial membrane potential were observed and evaluated under a fluorescent microscope (Nikon, Japan). In addition, mitochondria were isolated and purified according to the protocol provided by the mitochondrial extract kit (Solarbio Science & technology, Beijing, China). Western blotting was performed to examine Cytochrome C release from mitochondria.

Wound Healing Test

Wound healing (closure) tests were performed to assess the effects of EEFS on lung cancer cell migration. Briefly, NCI-H446 and NCI-H661 cells were seeded in 6-well plates. After scratching with a pipette tip, the floating cells were washed off with PBS and serum-free medium was added. Then, the cells were treated with EEFS (0, 0.1, 0.2, and 0.4 mg/ml for NCI-446 cells and 0, 0.125, 0.25, and

0.5 mg/ml for NCI-H661 cells) for 48 h. Cells were observed under a microscope and images of the scratches were taken at 0 h and 48 h after scratching. The wound closure width was measured by Image J software to calculate the difference in cell migration rate. Wound area was standardized using the following formula: wound closure rate (%) = ((initial wound area - wound area after 48 h) / initial wound area) × 100% [18].

Clonogenic Assays

The inhibitory effect of EEFS on the tumorigenicity of lung cancer cells was examined by clonogenic assay (colony formation test). NCI-H446 cells were inoculated into 6-well plates at a density of 1×10^3 cells/dish and treated with 0.1, 0.2, and 0.4 mg/ml EEFS for 48 h. Then, the cells were rinsed with PBS and new culture medium was added. After 14 days, culture medium was removed, and cells were rinsed with PBS. Cells were fixed with 4% paraformaldehyde and stained with 0.4 g/L crystal violet at room temperature for 15 min. Photos were taken and the colonies were counted.

Tumor Growth Inhibition Test

All animal experiments were conducted with a protocol approved by the animal care and use Committee of Shengjing Hospital of China Medical University. Male BALB/c-nu/nu nude mice, weighing between 14–16 g and aged from 4 to 6 weeks were reared in SPF (specific pathogen free) conditions with a 12 h light/12 h dark cycle and room temperature of 24–26 °C with a relative humidity of 50–60%. Nude mice were given standard feed and sterile drinking water. The mice were implanted with 5×10^6 NCI-H446 cells in 0.2 ml PBS in the armpit of the right forelimb. Tumor volume was assessed by measuring the length (L) and width (W) with Vernier calipers every other day. Tumor volume was calculated according to the following formula: tumor volume (mm^3) = $0.52 \times L \times W^2$. When the tumor volume reached 100 mm^3, the mice were randomly divided into two groups (n = 4). In the treatment group, 0.1 ml EEFS (200 mg/kg) was dissolved with 0.1% sodium carboxymethylcellulose (CMC-Na) and given by gavage daily for 26 days, the control group was gavaged with CMC-Na. At the end of the experiment, the animals were sacrificed by intraperitoneal injection of 150 mg/kg pentobarbital sodium. After photographing the mice, the tumors were excised and photographed. The tumors were weighed to calculate the average tumor mass. The tumor tissues were stored at − 80 °C for further analysis.

Statistical analysis

Graphpad prism 8.0 (San Diego, CA, USA) was used to analyze data. Student's t test was used to compare means between two groups, and one-way ANOVA followed by Dunnett’s test was used to compare means between multiple groups. A p value less than 0.05 was considered statistically significant.

Results

EEFS induced morphological changes in lung cancer cells

To investigate the cytotoxic effects of EEFS, NCI-H446 or NCI-H661 lung cancer cell lines were treated with different concentrations of EEFS for 48 h or the same concentration of EEFS for different time frames, as indicated. Morphological changes in adherent cells were observed and photographed using a phase contrast microscope. Results showed that 0.8 mg/ml (NCI-H446 cells, Fig. 1A and 1B) or 1 mg/ml (NCI-H661cells, Fig. 1C and 1D) EEFS resulted in adherent cells becoming round, shrinking, and separating from the bottom of the culture plate, all changes indicative of apoptosis. To further test the cytotoxicity of EEFS, DNA condensation or fragmentation in the cell nucleus was observed under fluorescence microscope using Hoechst 33258 fluorescent dye staining. Results demonstrated that 0.8 mg/ml (for NCI-H446 cells, Fig. 1D and 1E) or 1 mg/ml (for NCI-H661cells, Fig. 1F and 1G) resulted in the occurrence of apoptotic nuclei (apoptotic nuclei are lighter than non-apoptotic cell nuclei) in both lung cancer cell lines. These data suggest that EEFS is toxic to lung cancer cells in vitro in a time and concentration-dependent manner.

EEFs Inhibited Lung Cancer Cell Viability

To evaluate the effect of EEFS on cell proliferation, we treated NCI-H446 and NCI-H661 cells with different concentrations of EEFS (0, 0.25, 0.5, and 1 mg/ml) for 48 h, or with the same concentration of EEFS for different time frames (12, 24, and 48 h). After treatment, MTS assay was performed to assess cell viability. Results demonstrated that EEFS significantly reduced the viability of NCI-H446 (Fig. 2A and 2B) and NCI-H661 (Fig. 2C and 2D) cells in a time and dose dependent manner. When NCI-H446 cells were treated with 0.8 mg/ml EEFS, or NCI-H661 cells were treated with 1.0 mg/ml EEFS for 48 h, cell viability decreased to 27.9% and 34.87%, respectively. These data suggest that EEFS effectively inhibited the proliferation of lung cancer cells in vitro.

Quantitative Analysis Of EEFS-induced Apoptosis

To quantitatively analyze apoptosis induced by EEFS, NCI-H446 or NCI-H661 cells were treated with different concentrations of EEFS or the same concentration for various time frames, as indicated. After treatment, the cells were collected for Annexin V (FITC, green) - PI (Red) double staining and apoptosis was analyzed by flow cytometry. As shown in Fig. 3A, when NCI-H446 cells were treated with different concentrations of EEFS (0.2, 0.4, and 0.8 mg/ml), the apoptosis rate was 9.18%, 12.15%, and 88.05%, respectively, which was significantly higher than in the control group (7.55%). When NCI-H446 cells were treated with 0.8 mg/ml EEFS for different time periods (12, 24, and 48 h), the apoptosis rate was 29.16%, 54.22%, and 66.36%, respectively, which was significantly higher than in the control group (8.77%) (Fig. 3B). Similarly, the apoptosis rate in NCI-H661 cells was 6.69%, 15.9%, and 64.93% (Fig. 3C) after 48 h of treatment with 0.25, 0.5, and 1 mg/ml EEFS, respectively, which was significantly higher than in

the control (4.89%). When NCI-H661 were treated with 0.8 mg/ml EEFS for different time periods (12, 24, and 48 h), the apoptosis rate was 28.61%, 48.82%, and 63.43%, respectively, which was significantly higher than in the control group (5.83%) (Fig. 3D). These data suggest that EEFS effectively induced apoptosis in lung cancer cells.

EEFS Decreased Bcl-2 Protein Expression In Lung Cancer Cells

We next explored the mechanisms through which EEFS induced apoptosis by analyzing apoptosis-related protein expression or activation via Western blotting. NCI-H446 or NCI-H661 cells were treated with different concentrations of EEFS for 48 h or the same concentration of EEFS for different time periods, as indicated. The protein levels of cleaved Caspase 3, Bak, Bax, Bcl-2 and Survivin were examined. As shown in Fig. 4A (NCI-H446 cells) and 4B (NCI-H661 cells), EEFS-induced an increase in cleaved Caspase 3 in a time- and dose-dependent manner, implying that EEFS triggered apoptosis by activating the protease Caspase 3. Further detection revealed that expression of the anti-apoptotic proteins Bcl-2 and Survivin was down-regulated, while expression of the pro-apoptotic proteins Bak and Bax increased in both cell lines (Fig. 4C, NCI-H446 and Fig. 4D, NCI-H661). To further verify that EEFS induced apoptosis by inhibiting Bcl-2 expression, cells were left untreated or treated with a sub-lethal dose of the Bcl-2 inhibitor ABT-263, EEFS, or ABT-263 + EEFS. The protein levels of cleaved Caspase 3 and Bcl-2 were assessed. As shown in Fig. 4E (left panel), compared to the control, cleaved Caspase 3 was only elevated in the ABT-263 and EEFS co-treatment groups. In addition, NCI-H446 cells were treated with 0.1 μM ABT-263 plus 0.4 mg/ml EEFS for different time frames. Results showed that the addition of ABT-263 increased the effectiveness of EEFS in inducing Caspase 3 cleavage activation in NCI-H446 cells (Fig. 4E, right panel). This result indicated that EEFS may induce apoptosis by inhibiting Bcl-2.

EEFS Induced Mitochondrial Toxicity In Lung Cancer Cells

The Bcl-2 protein is essential for the maintenance of mitochondrial function [19]. To investigate whether the decrease of Bcl-2 induced by EEFS had an effect on mitochondria, we treated NCI-H446 cells with 0.8 mg/ml EEFS for different time points (0, 6, 12, and 24 h), stained them using Mito-tracker red probe, and observed the change in mitochondrial membrane potential. As shown in Fig. 5A, mitochondrial membrane potential decreased starting at 6 h and was mostly gone at 24 h. Next, we used Western blotting to measure Cytochrome C release from the mitochondria. NCI-H446 cells were treated with different concentrations of EEFS (0, 0.1, 0.2, 0.4, and 0.8 mg/ml), and mitochondria were purified. As shown in Fig. 5B, the Cytochrome C protein content in the mitochondria decreased gradually, while the content of Cytochrome C in the cytoplasm increased correspondingly. This indicated that EEFS may trigger Cytochrome C by inducing a decrease in mitochondrial membrane potential. These data suggest that EEFS may exert its cytotoxic effects by targeting the mitochondria.

EEFS Inhibited Lung Cancer Cell Migration

To evaluate the effects of EEFS on cell migration, NCI-H446 and NCI-H661 cells were treated with different concentrations of EEFS for 48 h, and cell migration was determined by measuring wound healing over time. Results showed that EEFS treatment significantly inhibited the migration of both lung cancer cell lines in a concentration dependent manner (Fig. 6A and 6B). These data show that EEFS can inhibit lung cancer cell migration.

EEFS Inhibited Colony Formation In Lung Cancer Cells

Colony formation is very important for tumorigenesis [20]. Therefore, we evaluated the effect of EEFS on the tumorigenicity of lung cancer cells via colony formation assay. After treatment with different concentrations of EEFS, the cells were stained with crystal violet and photographed. As shown in Fig. 7A (left panel), colony formation decreased as the concentration of EEFS increased. Compared with the control group, the amount of colony formation in the treatment group with 0.4 mg/ml EEFS decreased by 72.25% (Fig. 7, right panel). This data suggests that EEFS effectively inhibited colony formation in lung cancer cells.

EEFS Inhibited Lung Tumor Growth In Mice

Finally, we examined EEFS inhibition of tumor growth and its effects on Bcl2 and apoptosis in vivo. NCI-H446 cells were injected subcutaneously into nude mice and the inhibitory effect of oral gavage of EEFS on tumor growth was assessed. EEFS (200 mg/kg) or 0.1% CMC-Na as control was administered by gavage daily for 26 days to the lung cancer xenograft mice. As shown in Fig. 8A and 8C, the tumor volume of the EEFS-treated group was visibly smaller than that of the control group. The average increase in tumor volume in the EEFS treatment group was significantly lower than that of the control group (Fig. 8B). The average tumor weight in the EEFS treatment group was 3-fold lower than the control group (Fig. 8D). To analyze the effect of EEFS on Bcl-2 and Caspase-3 protein expression in lung cancer cells in vivo, the proteins from the above tumor samples were prepared for Western blotting. As shown in Fig. 8E, compared with the control group, the level of Bcl-2 protein in the EEFS group decreased while cleaved Caspase 3 activation increased. These data suggest that EEFS inhibited tumor growth in vivo by targeting Bcl-2-mediated apoptosis. Finally, we summarized the anti-lung cancer effects of EEFS in vitro and in vivo by a schematic diagram (Fig. 8F).

Discussion

Although there has been great progress in the screening, prevention, and treatment of lung cancer, it remains the cancer with the highest incidence and mortality rate, with a five year survival rate of less than 5% [21]. One main reason for the lethality of lung cancer is that there is currently no effective treatment regime for mid and advanced lung cancer, and most patients die due to uncontrolled distant metastasis

and recurrence [22, 23]. Compared with conventional chemotherapy drugs, such as platinum or paclitaxel, various new molecular targeted drugs such as tyrosine kinase inhibitors including Gefitinib and Erlotinib, or angiogenesis monoclonal antibodies, including Bevacizumab and Ramolumab, have been developed. Although these targeted drugs alone or in combination with conventional drugs have achieved some therapeutic effects, there remain impediments such as resistance, metastasis, and recurrence in the later stages of treatment [24, 25]. Therefore, a key issue in lung cancer management is to identify drugs with low toxicity and multiple targets. Here, we have provided fundamental evidence demonstrating that intragastric administration of EEFS effectively inhibited the growth of lung cancer xenograft tumors with no significant toxic side effects in tumor bearing mice. Our findings suggest that the extract has potential clinical application as a lung cancer treatment.

Fennel is widely grown all over the world, especially in Asia, and has long been considered a safe herbal medicine or condiment [26, 27]. Although various extracts from different parts of fennel have shown anticancer activity [12, 28, 29], many studies lack evidence of the detailed molecular mechanisms or in vivo verification. First, our study preliminarily showed that EEFS significantly decreased cell viability and induced apoptosis in two types of lung cancer cells in vitro. Cancer is a result of the infinite proliferation of cells (a loss of apoptosis)[30], and mitochondria play a key role in the regulation of the balance between cell viability and apoptosis [31]. Our mechanistic analysis revealed that EEFS induced mitochondrial toxicity, as 0.8 mg/ml of EEFS reduced the mitochondrial membrane potential within 6 h, and 0.2 mg of EEFS effectively induced mitochondrial release of Cytochrome C. Mitochondrial membrane potential and Cytochrome C are important to the maintenance of mitochondrial function, and the permeability of the mitochondrial outer membrane is mainly regulated by the Bcl-2 protein family [31]. In further examining the molecular mechanism of EEFS-induced mitochondrial Cytochrome C release as well as the decrease of membrane potential, we found that EEFS effectively decreased Bcl-2 protein expression and increased Bax and Bak pro-apoptotic protein expression. Therefore, the decrease of Bcl-2 may lead to the activation of Bax or Bak and migration to the mitochondria, subsequently decreasing membrane potential and the release of Cytochrome C. Thus, we hypothesized that EEFS may induce apoptosis by targeting Bcl-2. We then blocked the activity of Bcl-2 with ABT-263 and analyzed the effect on EEFS-induced apoptosis in lung cancer cells. As expected, a sub-lethal dose of ABT-263 effectively sensitized the cells to a sub-lethal dose of EEFS, indicating that inhibition of Bcl-2 activity is crucial for EEFS-induced apoptosis. These results are consistent with a report showing that ABT-263 inhibition of Bcl-2 enhanced lung cancer cell apoptosis induced by cisplatin or radiation [32]. Second, we confirmed that the EEFS induced apoptosis of lung cancer cells in vivo. Lung cancer cells were inoculated into nude mice subcutaneously to obtain a xenograft lung cancer mouse model. After continuous administration of EEFS (200 mg/kg) for 26 days, tumor growth was significantly reduced compared to controls. Therefore, oral administration of EEFS resulted in anti-lung cancer bioactivity. These results are consistent with the results showing that gavage of Ginkgo biloba exocarp extracts induced apoptosis in xenograft tumors derived from Lewis lung cancer cells [33]. Importantly, Western blotting data indicated that EEFS affected the tumor site following gastric absorption and induced apoptosis by inhibiting expression of the Bcl-2 protein and inducing Caspase 3 activation. Therefore, this is the first study to elucidate that oral EEFS

exerts anti-lung cancer activity by targeting the onco-protein Bcl-2. This result is relevant to lung cancer patients because in clinical samples, approximately 30% of non-small cell lung cancer tissues and more than 80% of small cell lung cancer tissues over-express Bcl-2 [34]. Clinical trials have also confirmed that reducing Bcl-2 expression can effectively improve the therapeutic outcomes of chemotherapy drugs such as paclitaxel or carboplatin in lung cancer[35]. Thus, the anti-lung cancer effect of EEFS through targeting Bcl-2 is worthy of further study. Third, treatment of lung cancer with various chemotherapeutic drugs often results in cancer cell metastasis, which leads to treatment failure. We further investigated whether EEFS can inhibit the migration and colony formation of lung cancer cells. Interestingly, the wound healing and colony formation data demonstrated that that EEFS not only inhibited lung cancer cell metastasis, but also reduced tumorigenesis. These findings are in agreement with a previous report that pomegranate juice and peel extracts inhibited migration and colony formation in prostate cancer cells [36].

Conclusions

Our data demonstrate that EEFS exhibits antitumor activity by inhibiting lung cancer cell viability, clone formation and migration, and by inducing apoptosis. This anticancer activity is achieved by decreasing Bcl-2 protein expression. EEFS can inhibit xenograft tumor growth following gastric administration (Fig. 8F). Therefore, EEFS has potential clinical applications as a drug for lung cancer treatment. This study had some limitations, such as the lack of further separation, purification, and extraction of effective components in EEFS. Thus, more in-depth tests are warranted.

Abbreviations

Ethanol extract of Foeniculum vulgare seeds, EEFS; Non-small cell lung cancer, NSCLC; Small cell lung cancer, SCLC; Epidermal growth factor receptor-tyrosine kinase inhibitor, EGFR-TKI; Interleukin, IL-6; Tumor necrosis factor α, TNF-α; Horseradish peroxidase, HRP; Phosphatidylserine, PS; Sodium dodecyl sulfate polyacrylamide gel electrophoresis, SDS-PAGE; polyvinylidene fluoride, PVDF; Tris-Buffered Saline Tween-20, TBST; enhanced chemiluminescence, ECL; bovine serum albumin, BSA; sodium carboxymethylcellulose, CMC-Na.

Declarations

Availability of data and materials

Not applicable.

Acknowledgements

Not applicable.

Funding

This work was partially supported by National Natural Science Foundation of China (No.81771947, No.31371425), Liaoning Provincial Natural Science Foundation of China (No.20180551061).

Author information

Xiangxuan Zhao and Zaiming Lu contributed equally to this work.

Affiliations

Department of Radiology, Shengjing Hospital of China Medical University, Shenyang 110004, LN, China

Weiwei Ke, Xiangxuan Zhao and Zaiming Lu

Contributions

Study design: XXZ and ZML; Data Collection: WWK and XXZ; Data analysis: WWK, XXZ, and ZML; Manuscript preparation: XXZ and ZML. All authors read and approved the final manuscript.

Corresponding authors

Correspondence to Xiangxuan Zhao or Zaiming Lu.

Ethics declarations

Ethics approval and consent to participate

This study was performed with approval from the animal care and use Committee of Shengjing Hospital of China Medical University. All Animal experiments complied with the national guidelines for the care and use of laboratory animals.

Consent for publication

Not applicable.

Conflicts of interest

The authors declare there are no conflicts of interest, financial or otherwise.

References

1. Schulze AB, Evers G, Kerkhoff A, Mohr M, Schliemann C, Berdel WE, et al. Future Options of Molecular-Targeted Therapy in Small Cell Lung Cancer. Cancers (Basel). 2019;11(5):e690.
2. Zhang C, Leighl NB, Wu YL, Zhong WZ. Emerging therapies for non-small cell lung cancer. J Hematol Oncol. 2019;12(1):45.

3. Yang S, Zhang Z, Wang Q. Emerging therapies for small cell lung cancer. J Hematol Oncol. 2019;12(1):47.
4. Xu Z, Zhang F, Zhu Y, Liu F, Chen X, Wei L, et al. Traditional Chinese medicine Ze-Qi-Tang formula inhibit growth of non-small-cell lung cancer cells through the p53 pathway. J Ethnopharmacol. 2019;234:180-8.
5. Ye YT, Zhong W, Sun P, Wang D, Wang C, Hu LM, et al. Apoptosis induced by the methanol extract of Salvia miltiorrhiza Bunge in non-small cell lung cancer through PTEN-mediated inhibition of PI3K/Akt pathway. J Ethnopharmacol. 2017;200:107-16.
6. Ferioli F, Giambanelli E, D'Antuono LF. Fennel (Foeniculum vulgare Mill. subsp. piperitum) florets, a traditional culinary spice in Italy: evaluation of phenolics and volatiles in local populations, and comparison with the composition of other plant parts. J Sci Food Agric. 2017;97(15):5369-80.
7. Senatore F, Oliviero F, Scandolera E, Taglialatela-Scafati O, Roscigno G, Zaccardelli M, et al. Chemical composition, antimicrobial and antioxidant activities of anethole-rich oil from leaves of selected varieties of fennel [Foeniculum vulgare Mill. ssp. vulgare var. azoricum (Mill.) Thell]. Fitoterapia. 2013;90:214-9.
8. Badgujar SB, Patel VV, Bandivdekar AH. Foeniculum vulgareMill: A Review of Its Botany, Phytochemistry, Pharmacology, Contemporary Application, and Toxicology. BioMed Research International. 2014;2014:1-32.
9. Villarini M, Pagiotti R, Dominici L, Fatigoni C, Vannini S, Levorato S, et al. Investigation of the cytotoxic, genotoxic, and apoptosis-inducing effects of estragole isolated from fennel (Foeniculum vulgare). J Nat Prod. 2014;77(4):773-8.
10. Singh B, Kale RK. Chemomodulatory action of Foeniculum vulgare (Fennel) on skin and forestomach papillomagenesis, enzymes associated with xenobiotic metabolism and antioxidant status in murine model system. Food Chem Toxicol. 2008;46(12):3842-50.
11. Levorato S, Dominici L, Fatigoni C, Zadra C, Pagiotti R, Moretti M, et al. In vitro toxicity evaluation of estragole-containing preparations derived from Foeniculum vulgare Mill. (fennel) on HepG2 cells. Food and chemical toxicology : an international journal published for the British Industrial Biological Research Association. 2018;111:616-22.
12. Syed FQ, Elkady AI, Mohammed FA, Mirza MB, Hakeem KR, Alkarim S. Chloroform fraction of Foeniculum vulgare induced ROS mediated, mitochondria-caspase-dependent apoptotic pathway in MCF-7, human breast cancer cell line. Journal of ethnopharmacology. 2018;218:16-26.
13. Elkady AI. Anethole Inhibits the Proliferation of Human Prostate Cancer Cells via Induction of Cell Cycle Arrest and Apoptosis. Anticancer Agents Med Chem. 2018;18(2):216-36.
14. Mousavi M, Zaiter A, Becker L, Modarressi A, Baudelaire E, Dicko A. Optimisation of phytochemical characteristics and antioxidative properties of Foeniculum vulgare Mill. seeds and Ocimum basilicum L. leaves superfine powders using new parting process. Phytochem Anal. 2020;31(2):154-63.

15. Kerekes D, Csorba A, Gosztola B, Nemeth-Zambori E, Kiss T, Csupor D. Furocoumarin Content of Fennel-Below the Safety Threshold. Molecules. 2019;24(15):e2844.
16. Wang J-Z, Huang B-S, Cao Y, Chen K-L, Li J. Anti-hepatoma activities of ethyl acetate extract from Ampelopsis sinica root. Oncology Reports. 2017;37(4):2227-36.
17. Wan LF, Shen JJ, Wang YH, Zhao W, Fang NY, Yuan X, et al. Extracts of Qizhu decoction inhibit hepatitis and hepatocellular carcinoma in vitro and in C57BL/6 mice by suppressing NF-kappaB signaling. Sci Rep. 2019;9(1):1415.
18. Mine M, Yamaguchi K, Sugiura T, Chigita S, Yoshihama N, Yoshihama R, et al. miR-203 Inhibits Frizzled-2 Expression via CD82/KAI1 Expression in Human Lung Carcinoma Cells. PLOS ONE. 2015;10(7):e0131350.
19. Aouacheria A, Cibiel A, Guillemin Y, Gillet G, Lalle P. Modulating mitochondria-mediated apoptotic cell death through targeting of Bcl-2 family proteins. Recent patents on DNA & gene sequences. 2007;1(1):43-61.
20. Ding DC, Liu HW, Chu TY. Interleukin-6 from Ovarian Mesenchymal Stem Cells Promotes Proliferation, Sphere and Colony Formation and Tumorigenesis of an Ovarian Cancer Cell Line SKOV3. Journal of Cancer. 2016;7(13):1815-23.
21. Greenlee RT, Murray T, Bolden S, Wingo PA. Cancer statistics, 2000. CA: a cancer journal for clinicians. 2000;50(1):7-33.
22. Blumenthal GM, Bunn PA, Jr., Chaft JE, McCoach CE, Perez EA, Scagliotti GV, et al. Current Status and Future Perspectives on Neoadjuvant Therapy in Lung Cancer. Journal of thoracic oncology : official publication of the International Association for the Study of Lung Cancer. 2018;13(12):1818-31.
23. Oberndorfer F, Mullauer L. Molecular pathology of lung cancer: current status and perspectives. Current opinion in oncology. 2018;30(2):69-76.
24. Cafarotti S, Lococo F, Froesh P, Zappa F, Andre D. Target Therapy in Lung Cancer. Advances in experimental medicine and biology. 2016;893:127-36.
25. Sculier JP, Berghmans T, Meert AP. Advances in target therapy in lung cancer. European respiratory review : an official journal of the European Respiratory Society. 2015;24(135):23-9.
26. Namavar Jahromi B, Tartifizadeh A, Khabnadideh S. Comparison of fennel and mefenamic acid for the treatment of primary dysmenorrhea. International journal of gynaecology and obstetrics: the official organ of the International Federation of Gynaecology and Obstetrics. 2003;80(2):153-7.
27. Uusitalo L, Salmenhaara M, Isoniemi M, Garcia-Alvarez A, Serra-Majem L, Ribas-Barba L, et al. Intake of selected bioactive compounds from plant food supplements containing fennel (Foeniculum vulgare) among Finnish consumers. Food chemistry. 2016;194:619-25.
28. Ghasemi M. Investigation of Compositions and Effect of Herbal Essential Oils Local Silybum Marianum, Foeniculum Vulgare and Glycyrrhiza Glabra on Cell Line of Stomach Cancer by MTT Assays in Ardabil, Iran. Journal of minimally invasive gynecology. 2015;22(6S):S166.
29. Lall N, Kishore N, Binneman B, Twilley D, van de Venter M, du Plessis-Stoman D, et al. Cytotoxicity of syringin and 4-methoxycinnamyl alcohol isolated from Foeniculum vulgare on selected human cell

lines. Natural product research. 2015;29(18):1752-6.

30. Hassan M, Watari H, AbuAlmaaty A, Ohba Y, Sakuragi N. Apoptosis and Molecular Targeting Therapy in Cancer. Biomed Res Int.2014:1-23.
31. Cosentino K, Garcia-Saez AJ. Mitochondrial alterations in apoptosis. Chemistry and physics of lipids. 2014;181:62-75.
32. Li H, Wang H, Deng K, Han W, Hong B, Lin W. The ratio of Bcl-2/Bim as a predictor of cisplatin response provides a rational combination of ABT-263 with cisplatin or radiation in small cell lung cancer. Cancer biomarkers : section A of Disease markers. 2019;24(1):51-9.
33. Cao C, Su Y, Han D, Gao Y, Zhang M, Chen H, et al. Ginkgo biloba exocarp extracts induces apoptosis in Lewis lung cancer cells involving MAPK signaling pathways. Journal of ethnopharmacology. 2017;198:379-88.
34. Daniel JC, Smythe WR. The role of Bcl-2 family members in non-small cell lung cancer. Seminars in thoracic and cardiovascular surgery. 2004;16(1):19-27.
35. Herbst RS, Frankel SR. Oblimersen Sodium (Genasense bcl-2 Antisense Oligonucleotide) A Rational Therapeutic to Enhance Apoptosis in Therapy of Lung Cancer. Clinical Cancer Research An Official Journal of the American Association for Cancer Research. 2004;10(12 Pt 2):4245s-8s.
36. Chaves FM, Pavan ICB, da Silva LGS, de Freitas LB, Rostagno MA, Antunes AEC, et al. Pomegranate Juice and Peel Extracts are Able to Inhibit Proliferation, Migration and Colony Formation of Prostate Cancer Cell Lines and Modulate the Akt/mTOR/S6K Signaling Pathway. Plant Foods Hum Nutr. 2020;75(1):54-62.

Figures

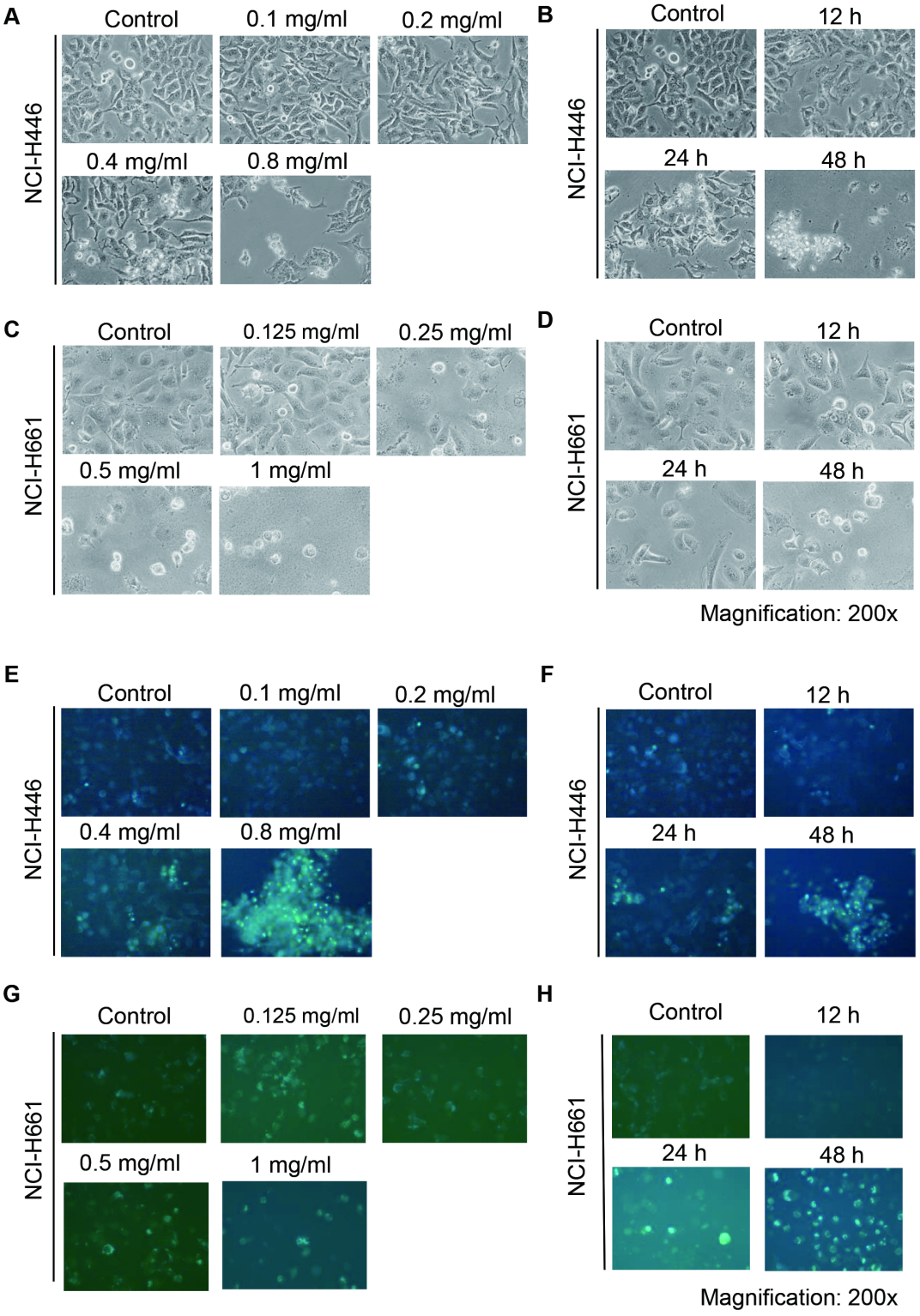

Figure 1

EEFS induced morphological changes in lung cancer cells. Cells were grown in 6-well plates with 5 × 105 cells per well. (A) NCI-H446 cells were treated with different concentrations of EEFS (0, 0.1, 0.2, 0.4, and 0.8 mg/ml) for 48 h. Phase contrast microscope was used to observe and photograph morphological changes in adherent cells (magnification: 200×). (B) NCI-H446 cells were treated with 0.8 mg/ml EEFS for different time points (0, 12, 24, and 48 h). Morphological changes were observed by phase contrast

microscope (magnification: 200×). (C) NCI-H661 cells were treated with different concentrations of EEFS (0, 0.125, 0.25, 0.5, and 1 mg/ml) for 48 h, and morphological changes were observed with a phase contrast microscope (magnification: 200×). (D) The morphological changes of NCI-H446 cells treated with 1 mg/ml EEFS at different times (0, 12, 24, and 48 h) were observed by phase contrast microscope (magnification: 200×). (E) NCI-H446 cells treated as in Fig. 1A were stained with Hoechst 33258 fluorescent dye to show nuclear morphological changes and to assess apoptosis (Apoptotic cells show condensed nuclei and fragmented DNA) (magnification: 200×). (F) NCI-H661cells were treated as in Fig. 1B. Apoptosis was assessed via nuclear morphological changes based on Hoechst 33258 staining to show cells with apoptotic nuclei (magnification: 200×). (G) NCI-H446 cells were treated as in Fig. 1C, then Hoechst 33258 was used to stain nuclei (magnification: 200×). (H) NCI-H661 cells were treated as in Fig. 1D. Apoptosis was determined by nuclear morphological changes based on Hoechst 33258 staining (magnification: 200×).

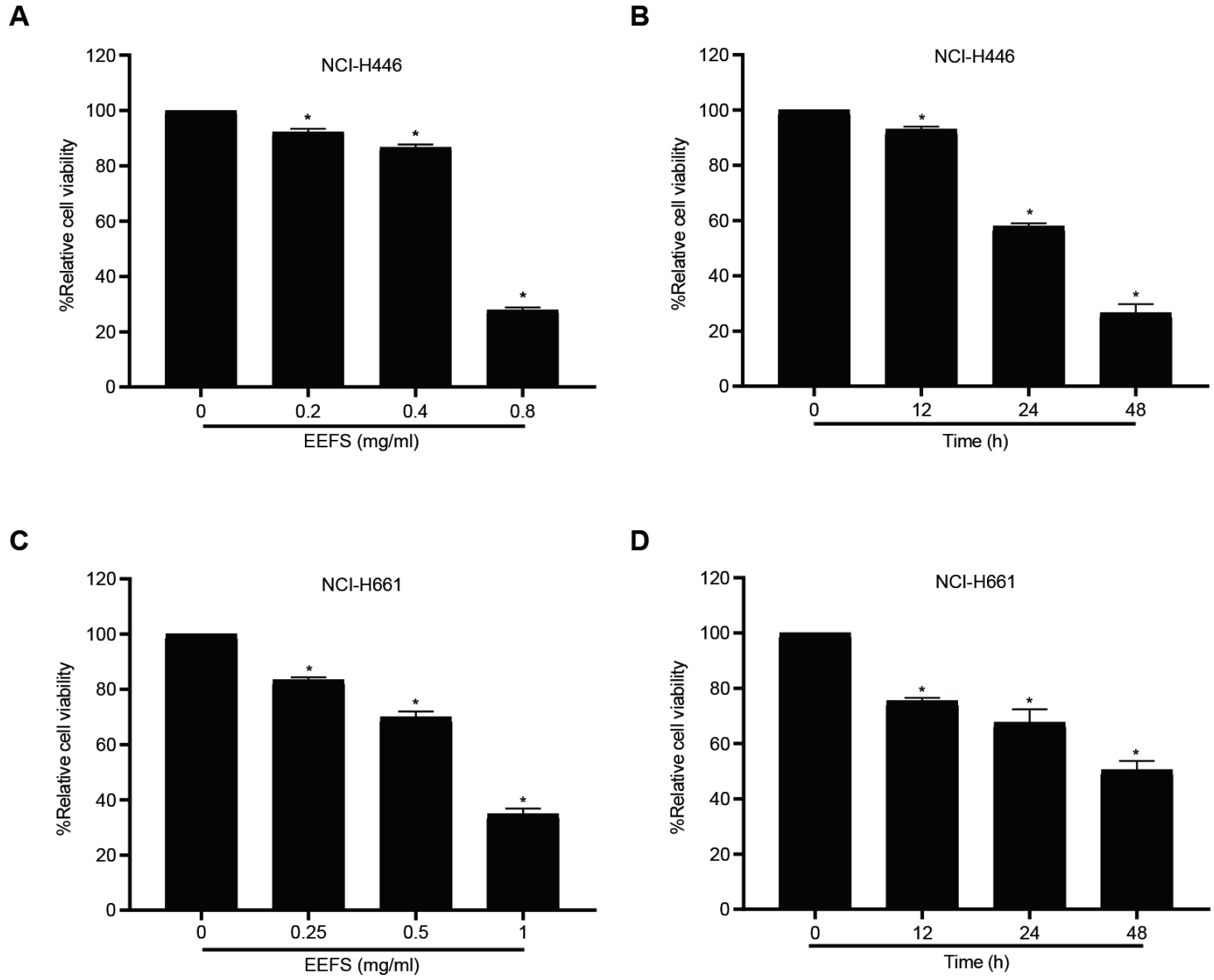

Figure 2

EEFS inhibited lung cancer cell viability. (A) NCI-H446 cells were grown in 96-well plates with 5 × 103 cells per well. Cells were treated with 0, 0.2, 0.4, and 0.8 mg/ml EEFS for 48 h. MTS was used to assess relative cell viability as described in Materials and Methods (*P < 0.05). (B) NCI-H446 cells were grown in 96-well plates with 5 × 103 cells per well. Cells were treated with 0.8 mg/ml EEFS for 0, 12, 24 and 48 h. Relative cell viability was examined by MTS assay (*P < 0.05). (C) NCI-H661 cells were grown in 96-well plates with 5 × 103 cells per well and treated with various concentrations of EEFS (0, 0.25, 0.5, and 1 mg/ml) for 48 h. Relative cell viability was assessed by MTS assay (*P < 0.05). (D) NCI-H661 cells were grown in 96-well plates with 5 × 103 cells per well. Cells were incubated with 1 mg/ml EEFS for 0, 12, 24, and 48 h. MTS assays were performed to test cell viability (*P < 0.05).

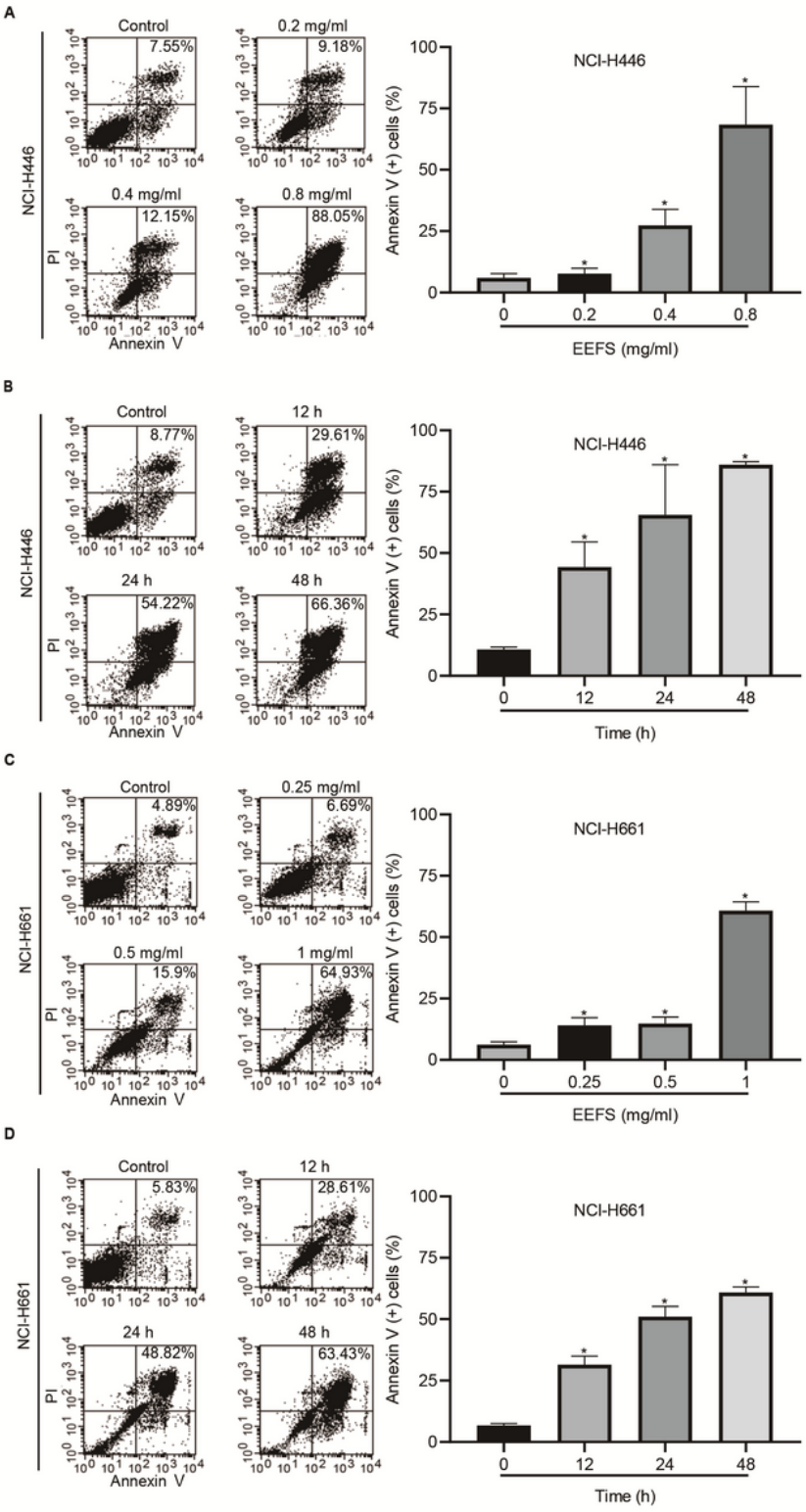

Figure 3

EEFS induced apoptosis in lung cancer cells. (A) NCI-H446 cells were grown in 6-well plates with 5 × 105 cells per well. Cells were treated with different concentrations of EEFS (0, 0.2, 0.4, and 0.8 mg/ml) for 48 h. Cells were harvested for Annexin V-PI double staining and subjected to flow cytometry (Left panel). Statistical analysis was performed to determine apoptotic ratio (Right panel, *P < 0.05). (B) NCI-H446 cells were grown in 6-well plates with 5 × 105 cells per well. Cells were treated with 0.8 mg/ml EEFS for

different times (0, 12, 24, and 48 h). After treatment, cells were harvested for Annexin V-PI double staining and apoptosis was analyzed through flow cytometry (Left panel). Statistical analysis was performed to determine apoptotic ratio (Right panel, *P < 0.05). (C) NCI-H661 cells were grown in 6-well plates with 5 × 105 cells per well. Cells were treated with different concentrations of EEFS (0, 0.25, 0.5, and 1 mg/ml) for 48 h. Flow cytometry to identify Annexin V-PI double staining was used to analyze apoptosis (Left panel). Statistical analysis was performed to determine the apoptotic ratio (Right panel, *P < 0.05). (D) NCI-H661 cell treatments with 1 mg/ml EEFS for different times (0, 12, 24, and 48 h) were harvested for Annexin V-PI double staining and apoptosis was analyzed through flow cytometry (Left panel). Statistical analysis was performed to determine apoptotic ratio (Right panel, *P < 0.05).

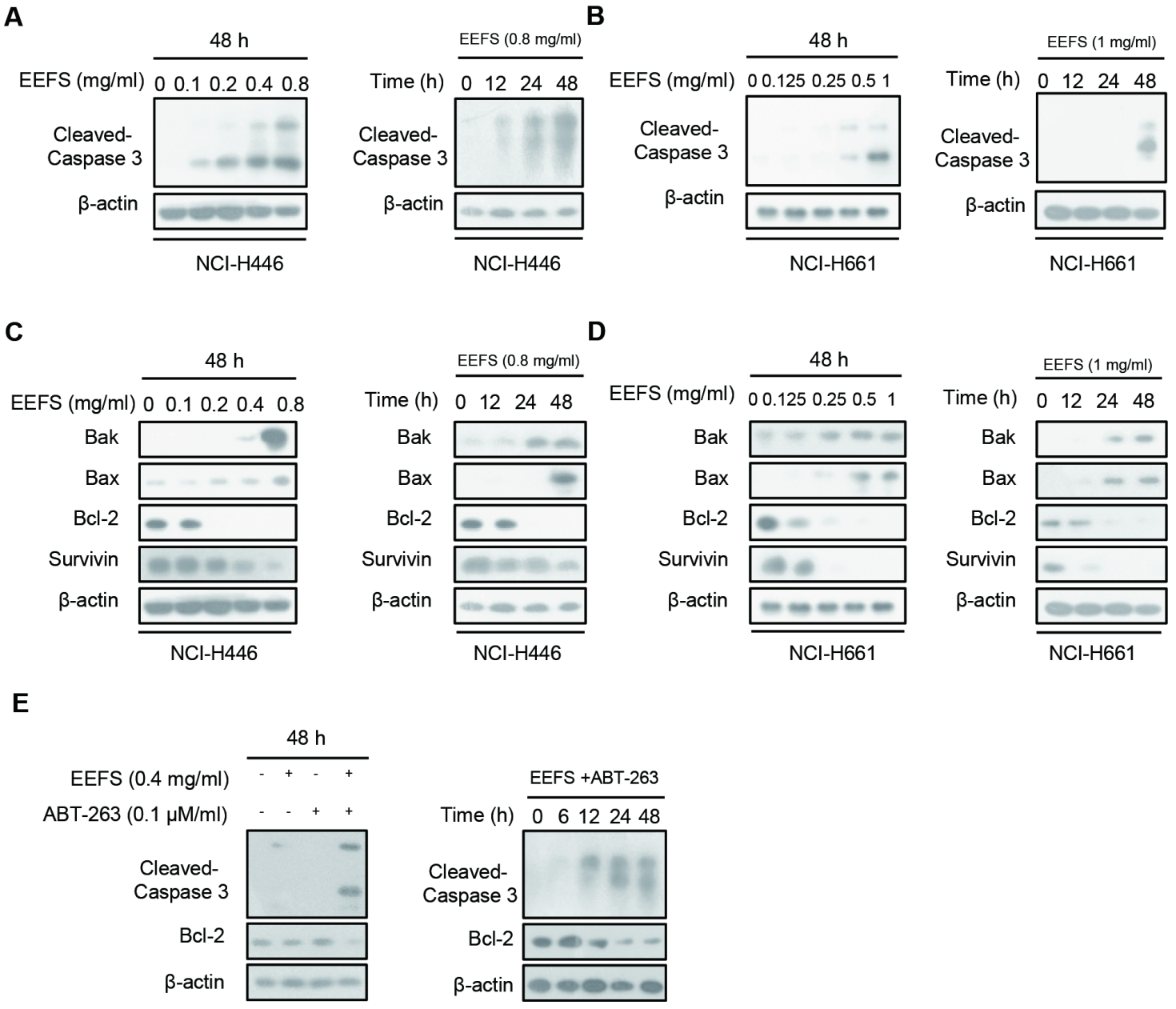

Figure 4

Effect of EEFS on apoptosis-related proteins in lung cancer cells. (A) NCI-H446 cells or (B) NCI-H661 cells were grown in 25 cm2 flasks with 5 × 106 cells. The cells were treated with EEFS (0, 0.1, 0.2, 0.4, and 0.8 mg/ml) for 48 h or 0.8 mg / ml for different time frames (0, 12, 24, and 48 h). Cells were harvested and subjected to Western blotting to assess cleaved Caspase 3 protein levels. β-actin was used as an internal control for equal protein loading. (C) NCI-H446 cells or (D) NCI-H661 cells were grown in 25 cm2 flasks with 5 × 106 cells. The cells were treated with EEFS (0, 0.1, 0.2, 0.4, and 0.8 mg/ml) for 48 h or 0.8 mg/ml for different time frames (0, 12, 24, and 48 h). At the end of various treatments, cells were harvested and subjected to Western blotting to assess protein levels of Bak, Bax, Bcl-2, and Survivin. β-actin was used as an internal control for equal protein loading. (E, right panel) NCI-H446 cells were grown in 25 cm2 flasks with 5 × 106 cells. Cells were untreated or treated with 0.1 μM ABT-263, 0.4 mg/ml EEFS or ABT-263 + EEFS for 48 h. Cells were harvested for Western blotting to analyze cleaved Caspase 3 and Bcl-2. β-actin was used as an internal control for equal protein loading. (E, left panel) NCI-H446 cells were grown in 25 cm2 flasks with 5 × 106 cells. Cells pretreated with 0.1 μM ABT-263 were incubated with 0.4 mg/ml EEFS for 0, 12, 24, and 48 h. Cells were harvested for Western blotting to analyze cleaved Caspase 3 and Bcl-2. β-actin was used as an internal control for equal protein loading.

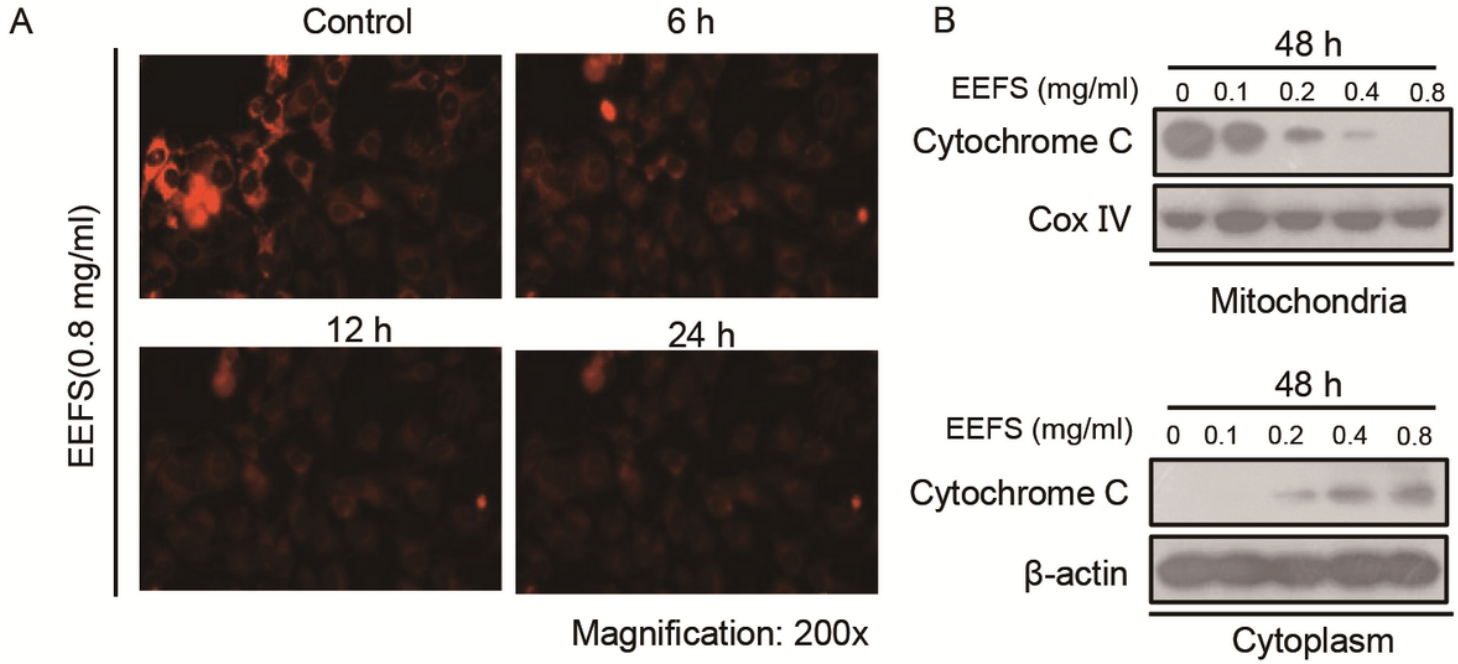

Figure 5

EEFS induced mitochondrial toxicity in lung cancer cells. (A) NCI-H446 cells were grown in 6-well plates with 4 × 105 cells per well. Cells were treated with EEFS (0, 0.1, 0.2, and 0.4 mg/ml) for 48 h, Mito-tracker red probe was directly added to the culture medium for mitochondria staining, and the change of membrane potential was observed by fluorescence microscope (magnification: 200×). (B) NCI-H446 cells were grown in 6-well plates with 4 × 105 cells per well. Cells were treated with EEFS (0, 0.1, 0.2, 0.4, and 0.8 mg/ml) for 48 h. Cells were harvested for mitochondrial purification and Western blotting was

performed to test Cytochrome C release. Cox-IV was used as an internal control for equal mitochondrial protein loading. β-actin was used as an internal control for equal cytosol protein loading.

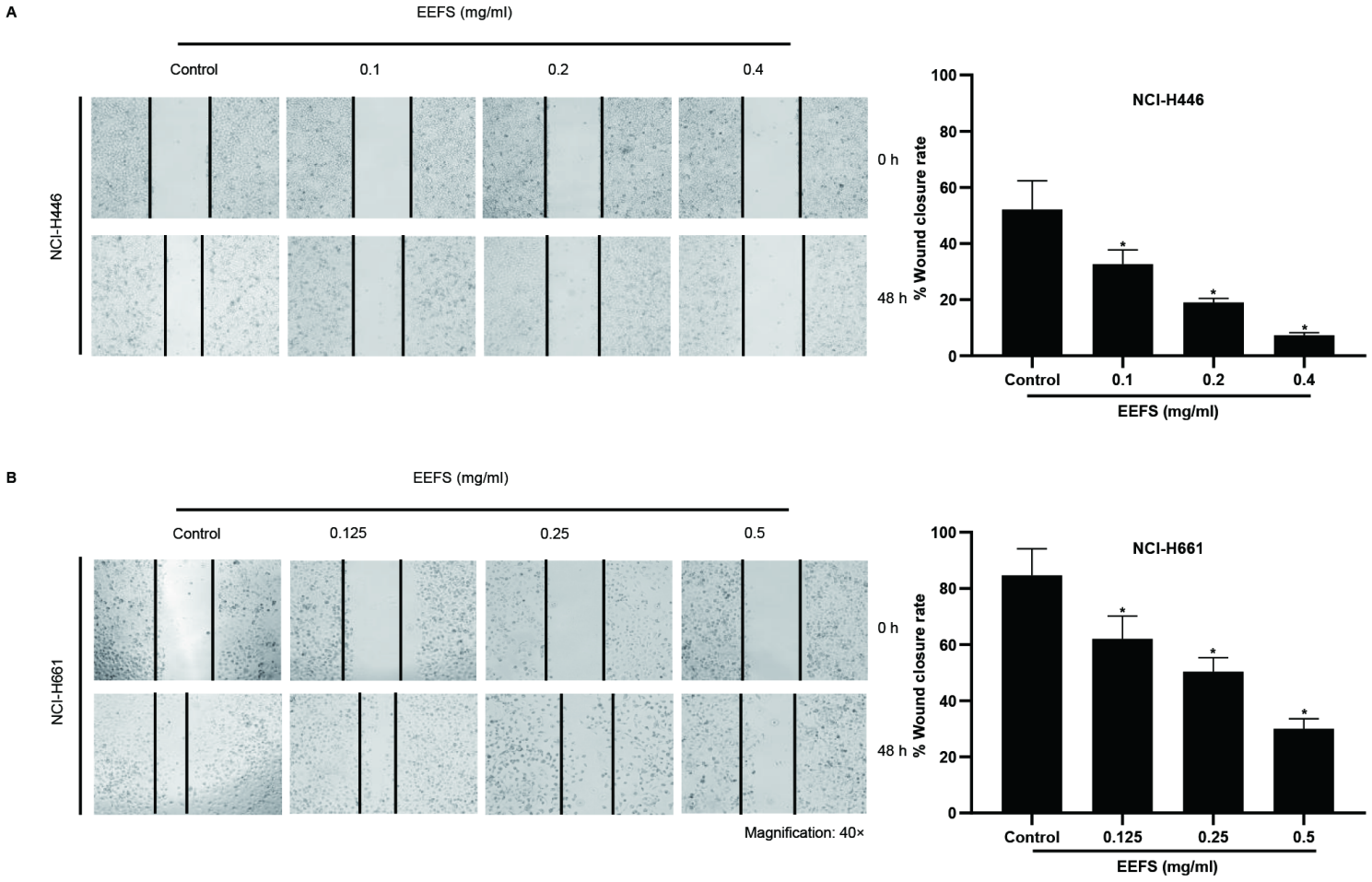

Figure 6

EEFS inhibited lung cancer cell migration. (A) NCI-H446 cells were seeded in 6-well plates with 1 × 106 cells per well. After scratching the bottom of the plate, cells were treated with 0, 0.1, 0.2 and 0.4 mg/ml EEFS. After 48 h, cells were photographed (left panel, magnification: 40×). The scratch width was measured to calculate the relative healing rate (Right panel, *P < 0.05). (B) NCI-H661 cells were seeded in 6-well plates. The bottom of the plate was scratched and cells were treated with 0, 0.125, 0.25 and 0.5 mg/ml EEFS for 48 h. After treatment, cells were photographed (Left panel, magnification: 40×). The scratch width was measured to calculate the relative healing rate (Right panel, *P < 0.05).

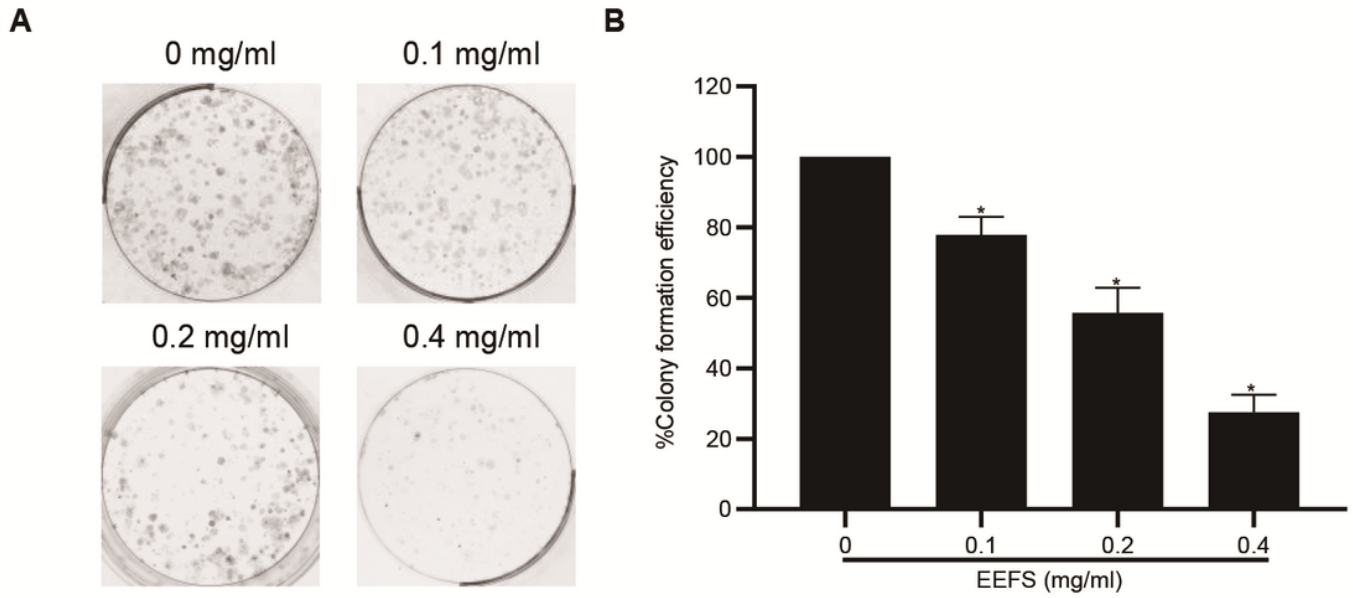

Figure 7

EEFS inhibited lung cancer cell colony formation. NCI-H446 cells were grown in 6-well plates with 1 × 103 cells per well. Cells were treated with 0, 0.1, 0.2, and 0.4 mg/ml EEFS for 48 h. Then, EEFS was removed by changing the culture medium and cells were cultured for another two weeks. (A) Crystal violet staining was performed to show cell colony formation (Left panel). (B) The cell colonies were counted, and statistical analysis was performed to evaluate the inhibition colony formation (Right panel, *P < 0.05).

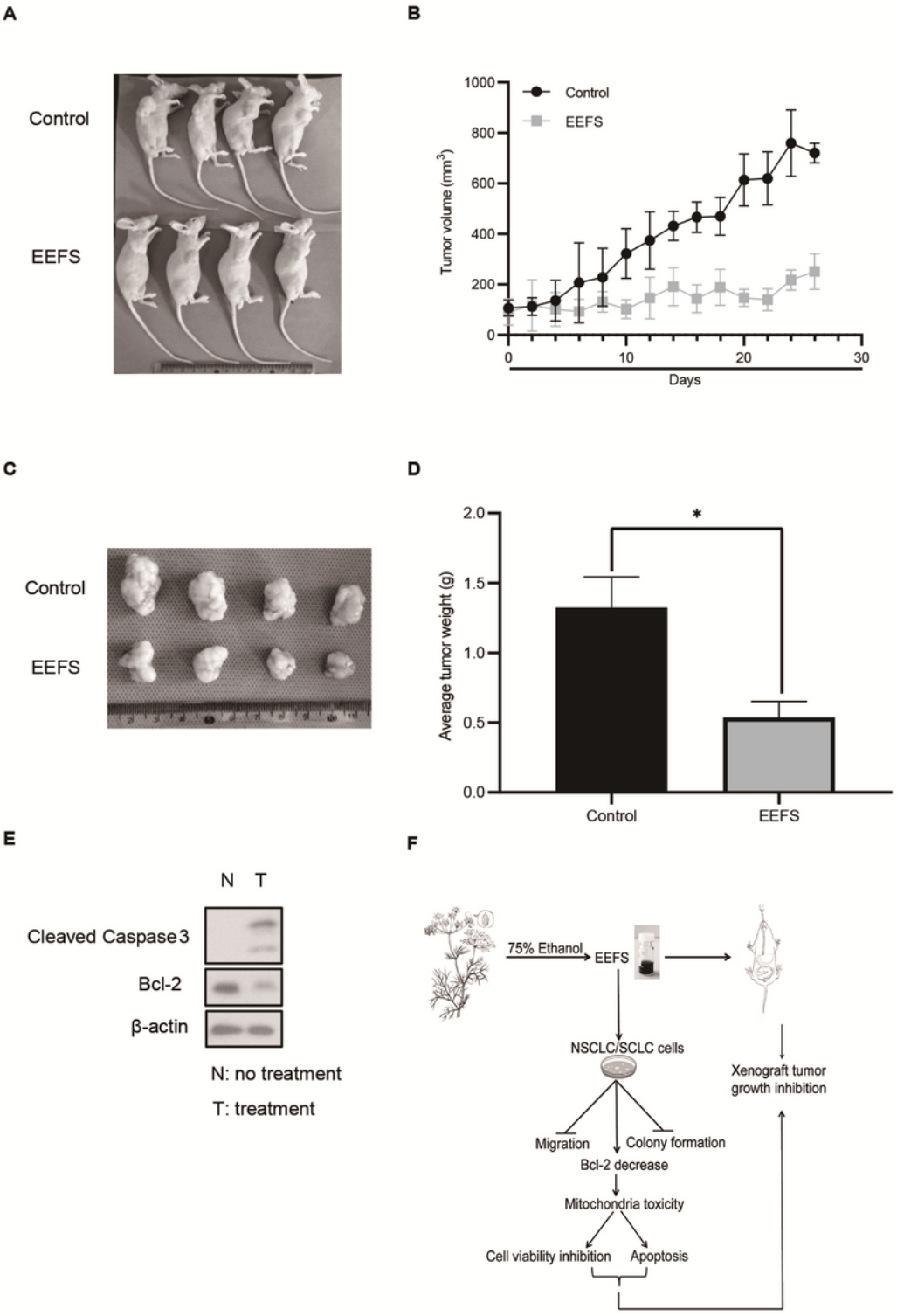

Figure 8

EEFS inhibited tumor growth in vivo. Lung cancer xenograft mice were gavaged with EEFS (200 mg/kg, n = 4) or given an equal volume of 0.1% CMC-Na (negative control, n = 4) daily for 26 days. Tumor volume and animal weight were measured daily during administration of EEFS or placebo. At the end of the experiment, the mice were sacrificed and photographed, then the tumors were dissected and photographed. (A) The EEFS treatment significantly inhibited the growth of lung cancer transplanted

tumors. (B) The tumor volume of the treatment group was lower than that of the control group. (C) The tumor size of the EEFS-treatment was smaller than that of the control group. (D) The average of tumor weight in the EEFS-treatment group was 3-fold less than that of the control group (*P < 0.05). (E) Tumor tissues from the control and EEFS groups were randomly selected, and the level of Bcl-2 and cleaved Caspase-3 proteins were measured by Western blotting. β-actin was used as an internal control for equal cytosolic protein loading. (F) Schematic diagram of the anti-lung cancer activity of EEFS: EEFS induced mitochondrial toxicity by targeting Bcl-2, leading to the inhibition of NSCLC and SCLC cell activity and apoptosis. Overall, antitumor activity was achieved by EEFS treatment in xenograft mice.